

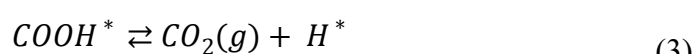
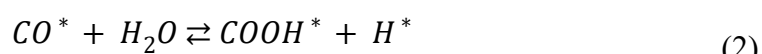
## Supplementary Information

### Rational design of highly efficient MXene-based catalysts for water-gas-shift reaction

Zhe Zhang<sup>ab</sup>, Baobing Zheng<sup>c</sup>, Hao Tian<sup>bd</sup>, Yanling He<sup>bd</sup>, Xiang Huang<sup>b</sup>, Sajjad Ali<sup>b</sup>, and Hu Hu<sup>bef\*</sup>

### Computational methods

To further confirm the effectiveness of water-assisted associative pathways for WGS reaction, a comprehensive microkinetic model is constructed on Au/M<sub>n+1</sub>X<sub>n</sub>O<sub>2</sub>. The micro-kinetic simulation of WGS reaction contains several basic reactions. All calculations are based on DFT thermodynamic and kinetic data. The turnover frequencies (TOF) and coverages simulated are the WGS reaction reach in a steady state. The surface coverages are constrained to sum to unity for each system. The corresponding elementary steps and reaction rates are as follows:



$$r_1 = k_1^+ P(CO)\theta_* - k_1^- \theta_{CO^*} \quad (5)$$

$$r_2 = k_2^+ P(H_2O)\theta_{CO^*} - k_2^- \theta_{COOH^*} \theta_{H^*} \quad (6)$$

$$r_3 = k_3^+ \theta_{COOH^*} - k_3^- P(CO_2)\theta_{H^*} \quad (7)$$

$$r_4 = k_4^+ \theta_{H^*}^2 - k_4^- P(H_2)\theta_*^2 \quad (8)$$

$$\frac{d}{d\theta} \theta_{CO^*} = r_1 - r_2 \quad (9)$$

$$\frac{d}{d\theta} \theta_{COOH^*} = r_2 - r_3 \quad (10)$$

$$\frac{d}{d\theta} \theta_{H^*} = r_2 + r_3 - 2r_4 \quad (11)$$

$$\frac{d}{d\theta} \theta_* = 2r_4 - r_1 \quad (12)$$

$$\sum_i \theta_i^* = 1 \quad (13)$$

Where  $\theta_i^*$  is coverage of the species. The  $k_1^+$  is the rate constant,  $k_1^-$  is the rate constant of the reverse reaction. Based on the transition state theory, the equilibrium constant ( $K_i$ ) and  $k_i$  of the chemical step i are given by:

$$K_i = \exp\left(-\frac{\Delta G_i}{k_B T}\right) \quad (14)$$

$$k_i = v_i \exp\left(-\frac{E_{a,i}}{k_B T}\right) \quad (15)$$

where  $\Delta G_i$ ,  $v_i$ , and  $E_{a,i}$  are the free energy change, pre-exponential factor, and activation energy of step i, respectively. Furthermore,  $k_B$  and  $T$  are the Boltzmann constant and temperature (298.15 K), respectively. For the reverse reactions,  $k_{-i}$  can be calculated through the equation:

$$k_{-i} = \frac{k_i}{K_i} \quad (16)$$

These equations have been numerically solved in the steady state. We have used them to further calculate the TOF. Under standard conditions, the free energy of the adsorbed hydrogen ( $\Delta G_{H^*}$ ) can be written as

$$\Delta G_{H^*} = \Delta E_{H^*} + \Delta E_{ZPE} - T\Delta S \quad (17)$$

$\Delta E_{ZPE}$  and  $T\Delta S$  are the differences of zero-point energy and entropy between the adsorbed hydrogen and hydrogen in the gas phase, respectively. The asterisk denotes the adsorption sites.  $\Delta E_{H^*}$  is the hydrogen chemisorption energy and is defined as

$$\Delta E_{H^*} = E_{nH^*} - E_{(n-1)H^*} - \frac{1}{2}E_{H_2(g)} \quad (18)$$

where  $E_{nH^*}$  and  $E_{(n-1)H^*}$  represent the total energies of the catalyst with n and n-1 adsorbed hydrogen atoms, respectively.  $E_{H_2(g)}$  represents the total energy of  $H_2$  in the gas phase. When  $\Delta G_{H^*}$  is less than 0, the proton transfer process is exothermic.

The free energy for all reaction intermediates is calculated as:

$$\Delta G^i = E_{DFT}^i + E_{ZPE}^i - TS^i \quad (19)$$

$E_{DFT}^i$  is the ground state potential energy obtained from DFT,  $E_{ZPE}^i$  is the zero-point energy, and  $TS^i$  is the entropy of the intermediate. Table S13 provides the free energies, zero-point energy, and entropy corrections used for the WGS intermediates.

The adsorption energy ( $E_{ad}$ ) is defined as

$$E_{ad} = E_{system} - (E_{adsorbent} + E_{adsorbate}) \quad (20)$$

where  $E_{system}$ ,  $E_{adsorbent}$ , and  $E_{adsorbate}$  are the total energies of the slab structure with the adsorbent, the adsorbent, and the slab structure, respectively.

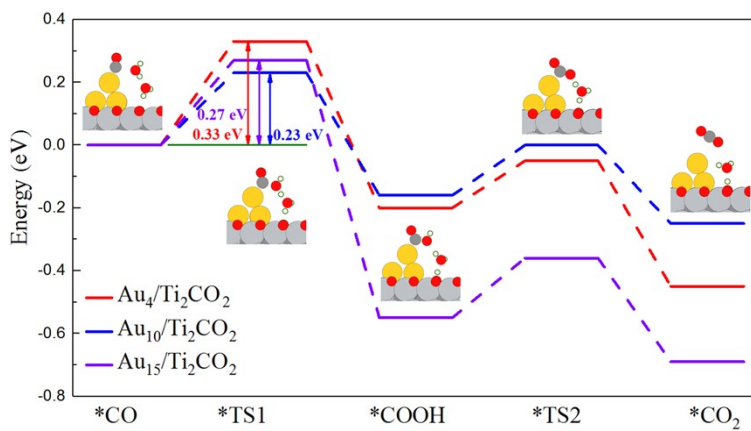


Fig. S1. Potential energy diagram for CO reforming via two H-bonded water molecules on  $\text{Au}_4/\text{Ti}_2\text{CO}_2$ ,  $\text{Au}_{10}/\text{Ti}_2\text{CO}_2$ , and  $\text{Au}_{15}/\text{Ti}_2\text{CO}_2$ . The activation barriers for  $*\text{CO} \rightarrow *\text{COOH}$  reforming are the rate-determining steps.

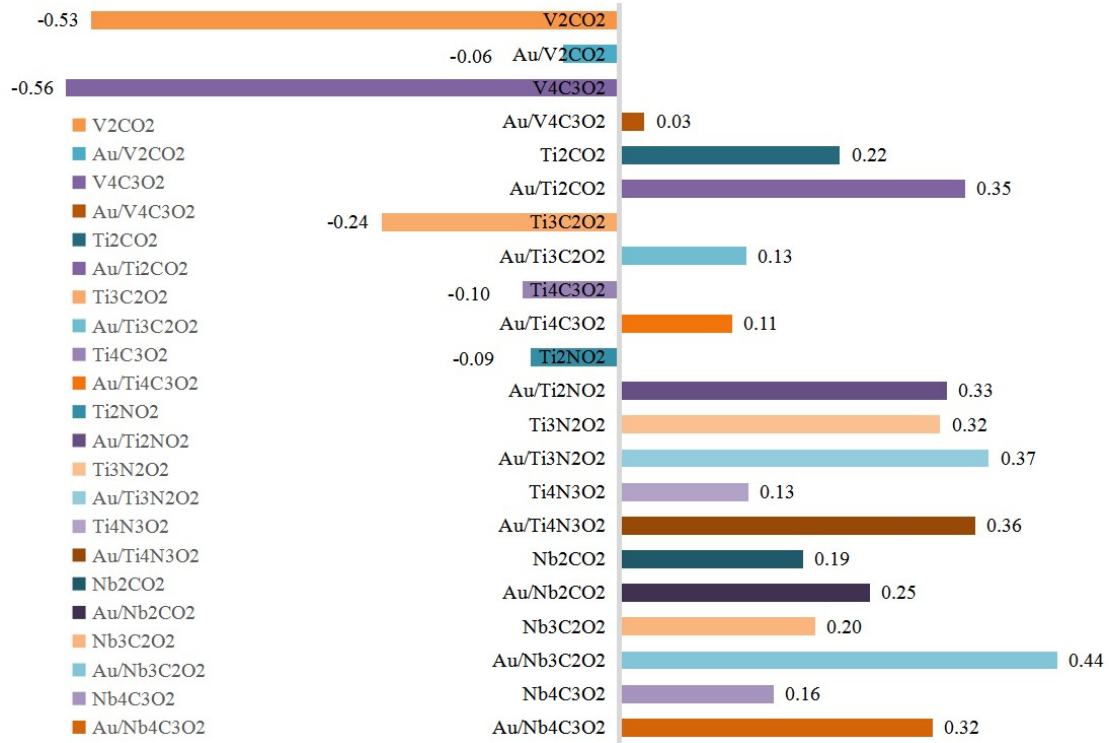


Fig. S2. The calculated free energies of H for surface O-termination MXene ( $M_{n+1}X_nO_2$ ) and MXene-supported Au clusters ( $Au/M_{n+1}X_nO_2$ ).

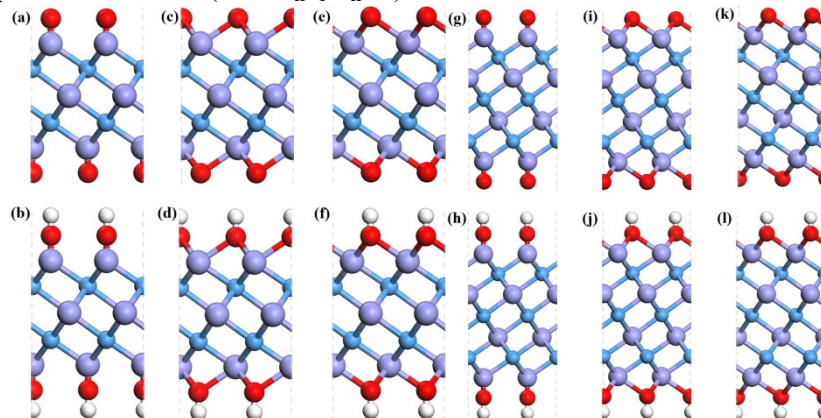


Fig. S3. Side views of three typical functionalized structures for  $M_3X_2T_2$  and  $M_4X_3T_2$  in a  $2 \times 2$  supercell. All the functional groups are located (a, b, g, h) on the top sites of the first layer of transition metals, (c, d, i, j) on the top of hexagonal close-packed (hcp) sites among the neighboring C/N atoms, and (e, f, k, l) above the face-centered-cubic (fcc) sites of the second layer of transition metal atoms. Purple, blue, red, and white spheres denote transitional metals, C/N atoms, functionalized O/F atoms, and H atoms, respectively.

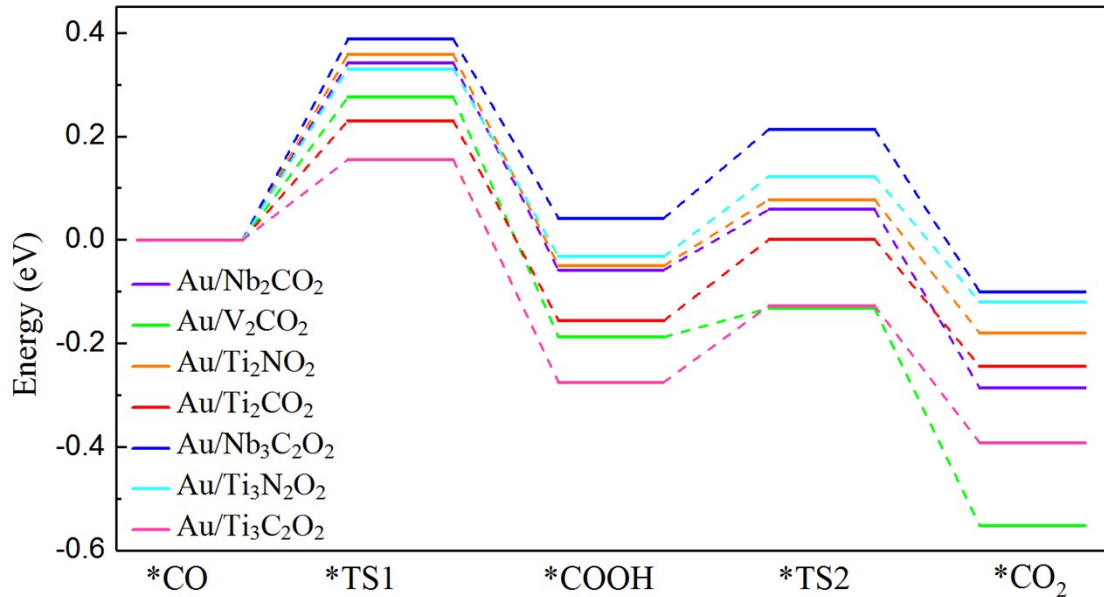


Fig. S4. Potential energy diagram for CO reforming via two H-bonded water molecules on  $\text{Au}/\text{M}_2\text{XO}_2$  and  $\text{Au}/\text{M}_3\text{X}_2\text{O}_2$ . The activation barriers for  $*\text{CO} \rightarrow *\text{COOH}$  reforming are the rate determining steps.

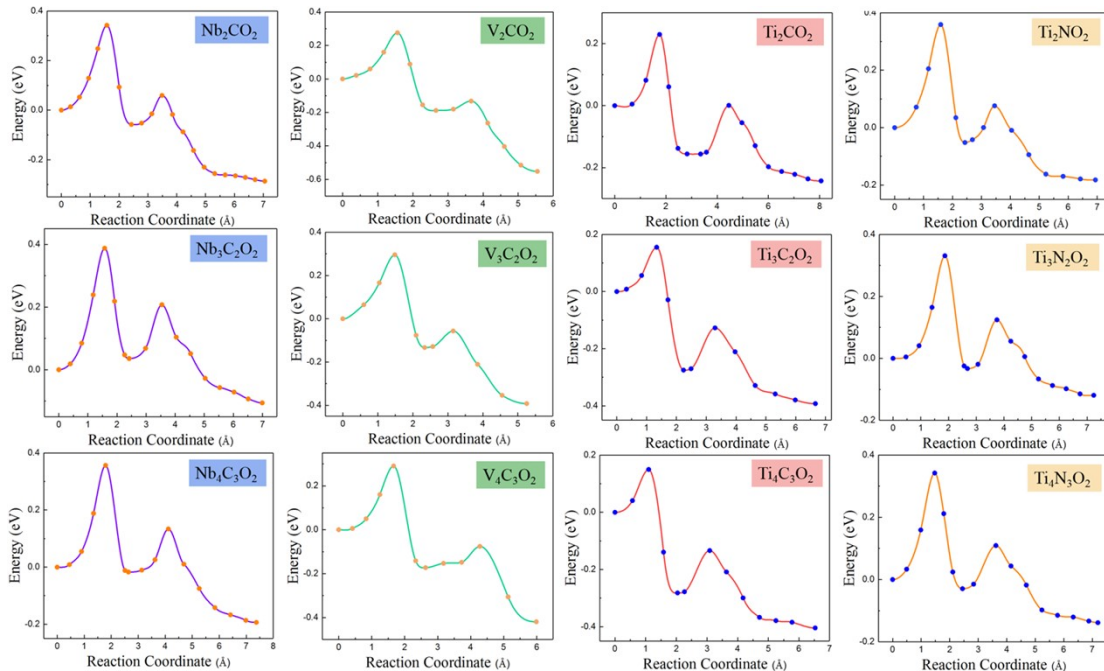


Fig. S5. Potential energy profiles for CO reforming via two H-bonded water molecules on  $\text{Au}/\text{M}_2\text{XO}_2$ ,  $\text{Au}/\text{M}_3\text{X}_2\text{O}_2$  and  $\text{Au}/\text{M}_4\text{X}_3\text{O}_2$ . The first peak in all figures is  $*\text{CO} \rightarrow *\text{COOH}$  reforming barrier, which is also the rate determining barrier. The second peak is the barrier for depositing the second  $*\text{H}$ , which is smaller than the former.

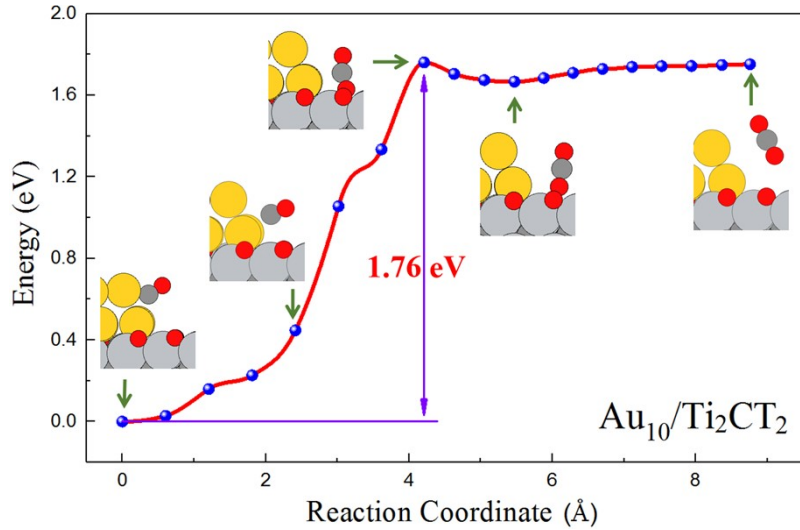


Fig. S6. Potential energy profile for CO binding O atom from the support and forming CO<sub>2</sub>.

Table S1. The calculated lattice constants and the total energies per unit cell for all the models of MXene are summarized. The lattices and energies of the most stable models are highlighted by overstriking.

MXene	Top site		Hcp site		Fcc site	
	lattice	Energy(eV)	lattice	Energy(eV)	lattice	Energy(eV)
Nb <sub>2</sub> CO <sub>2</sub>	3.12	-44.18	3.05	-47.37	<b>3.13</b>	<b>-47.94</b>
Nb <sub>2</sub> C(OH) <sub>2</sub>	3.19	-52.70	3.05	-53.81	<b>3.21</b>	<b>-53.86</b>
Nb <sub>2</sub> CF <sub>2</sub>	3.20	-40.58	3.01	-41.60	<b>3.20</b>	<b>-41.81</b>
Nb <sub>3</sub> C <sub>2</sub> O <sub>2</sub>	3.30	-65.23	3.08	-67.79	<b>3.15</b>	<b>-68.33</b>
Nb <sub>3</sub> C <sub>2</sub> (OH) <sub>2</sub>	3.19	-73.42	<b>3.09</b>	<b>-74.64</b>	3.12	-73.93
Nb <sub>3</sub> C <sub>2</sub> F <sub>2</sub>	3.21	-61.35	<b>3.07</b>	<b>-62.39</b>	3.11	-61.81
Nb <sub>4</sub> C <sub>3</sub> O <sub>2</sub>	3.13	-88.70	3.12	-88.52	<b>3.15</b>	<b>-88.97</b>
Nb <sub>4</sub> C <sub>3</sub> (OH) <sub>2</sub>	3.17	-94.08	<b>3.12</b>	<b>-95.11</b>	3.16	-94.80
Nb <sub>4</sub> C <sub>3</sub> F <sub>2</sub>	3.17	-82.00	<b>3.10</b>	<b>-82.84</b>	3.16	-82.75
V <sub>2</sub> CO <sub>2</sub>	3.05	-42.22	2.83	-43.78	<b>2.90</b>	<b>-44.41</b>
V <sub>2</sub> C(OH) <sub>2</sub>	3.18	-50.36	2.85	-50.96	<b>3.00</b>	<b>-51.21</b>
V <sub>2</sub> CF <sub>2</sub>	3.19	-38.29	2.80	-38.82	<b>2.98</b>	<b>-39.16</b>
V <sub>3</sub> C <sub>2</sub> O <sub>2</sub>	3.10	-61.48	2.87	-62.76	<b>2.92</b>	<b>-63.40</b>
V <sub>3</sub> C <sub>2</sub> (OH) <sub>2</sub>	3.03	-69.56	2.89	-70.24	<b>3.00</b>	<b>-69.91</b>
V <sub>3</sub> C <sub>2</sub> F <sub>2</sub>	3.04	-57.44	<b>2.86</b>	<b>-58.07</b>	2.96	-57.92
V <sub>4</sub> C <sub>3</sub> O <sub>2</sub>	3.06	-80.28	2.90	-81.95	<b>2.92</b>	<b>-82.53</b>
V <sub>4</sub> C <sub>3</sub> (OH) <sub>2</sub>	2.99	-88.62	<b>2.90</b>	<b>-89.32</b>	2.95	-89.19
V <sub>4</sub> C <sub>3</sub> F <sub>2</sub>	2.99	-76.48	2.88	-77.11	<b>2.94</b>	<b>-77.19</b>
Ti <sub>2</sub> NO <sub>2</sub>	3.00	-45.98	2.90	-44.71	<b>3.01</b>	<b>-45.98</b>
Ti <sub>2</sub> N(OH) <sub>2</sub>	3.00	-49.55	2.95	-51.71	<b>3.05</b>	<b>-51.99</b>
Ti <sub>2</sub> NF <sub>2</sub>	3.08	-38.10	2.91	-39.65	<b>3.06</b>	<b>-40.07</b>
Ti <sub>3</sub> N <sub>2</sub> O <sub>2</sub>	3.01	-65.69	2.96	-64.44	<b>3.01</b>	<b>-65.69</b>
Ti <sub>3</sub> N <sub>2</sub> (OH) <sub>2</sub>	3.02	-71.36	<b>2.97</b>	<b>-71.50</b>	3.02	-71.36

<i>Ti<sub>3</sub>N<sub>2</sub>F<sub>2</sub></i>	<b>3.13</b>	-57.89	<b>2.94</b>	<b>-59.48</b>	3.03	-59.38
<i>Ti<sub>4</sub>N<sub>3</sub>O<sub>2</sub></i>	2.99	-79.13	2.97	-84.14	<b>3.00</b>	<b>-85.31</b>
<i>Ti<sub>4</sub>N<sub>3</sub>(OH)<sub>2</sub></i>	3.02	-91.15	2.98	-91.14	<b>3.02</b>	<b>-91.15</b>
<i>Ti<sub>4</sub>N<sub>3</sub>F<sub>2</sub></i>	2.99	-79.13	2.96	-79.05	<b>3.02</b>	<b>-79.22</b>
<i>Ti<sub>2</sub>CO<sub>2</sub></i>	3.10	-44.95	2.96	-43.20	<b>3.03</b>	<b>-45.04</b>
<i>Ti<sub>2</sub>C(OH)<sub>2</sub></i>	3.05	-51.38	3.02	-51.06	<b>3.07</b>	<b>-51.39</b>
<i>Ti<sub>2</sub>CF<sub>2</sub></i>	3.21	-37.87	2.98	-38.98	<b>3.06</b>	<b>-39.52</b>
<i>Ti<sub>3</sub>C<sub>2</sub>O<sub>2</sub></i>	3.04	-63.67	3.03	-62.16	<b>3.04</b>	<b>-63.67</b>
<i>Ti<sub>3</sub>C<sub>2</sub>(OH)<sub>2</sub></i>	3.08	-70.20	3.04	-69.70	<b>3.09</b>	<b>-70.20</b>
<i>Ti<sub>3</sub>C<sub>2</sub>F<sub>2</sub></i>	3.16	-56.79	3.02	-57.63	<b>3.08</b>	<b>-58.37</b>
<i>Ti<sub>4</sub>C<sub>3</sub>O<sub>2</sub></i>	3.04	-82.40	3.03	-80.86	<b>3.04</b>	<b>-82.40</b>
<i>Ti<sub>4</sub>C<sub>3</sub>(OH)<sub>2</sub></i>	3.09	-88.84	3.05	-88.36	<b>3.09</b>	<b>-88.84</b>
<i>Ti<sub>4</sub>C<sub>3</sub>F<sub>2</sub></i>	3.15	-75.52	3.03	-76.27	<b>3.08</b>	<b>-77.01</b>

Table S2. The calculated lattice constants and the total energies per unit cell for bare MXene are summarized.

<i>MXene</i>	<i>lattice</i>	<i>Energy(eV)</i>	<i>MXene</i>	<i>lattice</i>	<i>Energy(eV)</i>
<i>Nb<sub>2</sub>C</i>	3.12	-28.71	<i>V<sub>2</sub>C</i>	2.89	-26.31
<i>Ti<sub>2</sub>N</i>	2.97	-25.75	<i>Ti<sub>2</sub>C</i>	3.07	-25.03
<i>Nb<sub>3</sub>C<sub>2</sub></i>	3.15	-49.34	<i>V<sub>3</sub>C<sub>2</sub></i>	2.95	-45.67
<i>Ti<sub>3</sub>N<sub>2</sub></i>	2.99	-45.35	<i>Ti<sub>3</sub>C<sub>2</sub></i>	3.09	-43.97
<i>Nb<sub>4</sub>C<sub>3</sub></i>	3.13	-70.21	<i>V<sub>4</sub>C<sub>3</sub></i>	2.92	-64.85
<i>Ti<sub>4</sub>N<sub>3</sub></i>	2.99	-65.19	<i>Ti<sub>4</sub>C<sub>3</sub></i>	3.10	-62.68

Table S3. The binding energies of functional groups T = O, OH, and F at the most stable sites on MXene surfaces.

<i>MXene</i>	<i>E<sub>O</sub> (eV)</i>	<i>O site</i>	<i>E<sub>OH</sub> (eV)</i>	<i>OH site</i>	<i>E<sub>F</sub> (eV)</i>	<i>F site</i>
<i>Nb<sub>2</sub>CT<sub>2</sub></i>	<b>-2.17</b>	<i>fcc</i>	-1.74	<i>fcc</i>	-2.06	<i>fcc</i>
<i>Nb<sub>3</sub>C<sub>2</sub>T<sub>2</sub></i>	<b>-2.05</b>	<i>fcc</i>	-1.82	<i>hcp</i>	-2.03	<i>hcp</i>
<i>Nb<sub>4</sub>C<sub>3</sub>T<sub>2</sub></i>	<b>-1.93</b>	<i>fcc</i>	-1.62	<i>hcp</i>	-1.82	<i>hcp</i>
<i>Ti<sub>2</sub>NT<sub>2</sub></i>	<b>-2.67</b>	<i>fcc</i>	-2.29	<i>fcc</i>	-2.66	<i>fcc</i>
<i>Ti<sub>3</sub>N<sub>2</sub>T<sub>2</sub></i>	<b>-2.72</b>	<i>fcc</i>	-2.24	<i>hcp</i>	-2.57	<i>hcp</i>
<i>Ti<sub>4</sub>N<sub>3</sub>T<sub>2</sub></i>	<b>-2.61</b>	<i>fcc</i>	-2.15	<i>fcc</i>	-2.52	<i>fcc</i>
<i>V<sub>2</sub>CT<sub>2</sub></i>	-1.62	<i>fcc</i>	-1.60	<i>fcc</i>	<b>-1.93</b>	<i>fcc</i>
<i>V<sub>3</sub>C<sub>2</sub>T<sub>2</sub></i>	-1.42	<i>fcc</i>	-1.29	<i>fcc</i>	<b>-1.71</b>	<i>hcp</i>
<i>V<sub>4</sub>C<sub>3</sub>T<sub>2</sub></i>	-1.40	<i>fcc</i>	-1.39	<i>hcp</i>	<b>-1.68</b>	<i>fcc</i>
<i>Ti<sub>2</sub>CT<sub>2</sub></i>	-2.56	<i>fcc</i>	-2.35	<i>fcc</i>	<b>-2.75</b>	<i>fcc</i>
<i>Ti<sub>3</sub>C<sub>2</sub>T<sub>2</sub></i>	-2.40	<i>fcc</i>	-2.28	<i>fcc</i>	<b>-2.71</b>	<i>fcc</i>
<i>Ti<sub>4</sub>C<sub>3</sub>T<sub>2</sub></i>	-2.41	<i>fcc</i>	-2.25	<i>fcc</i>	<b>-2.67</b>	<i>fcc</i>

Table S4. Calculated activation barriers and reaction energies of WGS reaction for different sizes and shape of Au clusters on Ti<sub>2</sub>CO<sub>2</sub>.

MXene	$*CO \rightarrow *COOH$		$*COOH \rightarrow *CO_2$	
	$E_{a_1}$ (eV)	$\Delta E_1$ (eV)	$E_{a_2}$ (eV)	$\Delta E_2$ (eV)
$Au_4/Ti_2CO_2$	0.33	-0.20	0.15	-0.25
$Au_{10}/Ti_2CO_2$	0.23	-0.16	0.16	-0.09
$Au_{15}/Ti_2CO_2$	0.27	-0.55	0.19	-0.14
$*CO \rightarrow *CO_2$				
$E_{a_1}$ (eV)		$\Delta E_1$ (eV)		
$Au_{10}/Ti_2CO_2$	1.76	1.67		

Table S5. The CO adsorption energies at different sites of  $Au_4$ ,  $Au_{10}$ , and  $Au_{15}$  clusters on  $Ti_2CO_2$ .

Top view	Side view	$E_{CO}$ (eV)	Top view	Side view	$E_{CO}$ (eV)	Top view	Side view	$E_{CO}$ (eV)
		-0.51			-0.71			-0.65
		-0.42			-0.50			-0.59
		-0.03			-0.40			-0.29
		-0.01			-0.01			-0.01

Table S6. The geometric structures of  $Au_{10}$  clusters and the adsorption energies of per Au atom for  $Au_{10}$  cluster on  $Ti_2CO_2$ .

Geometric structures	Top view	Side view	Adsorption Energy (eV)
$Au_{10}$ cluster-1			-0.80
$Au_{10}$ cluster-2			-0.78
$Au_{10}$ cluster-3			-0.76
$Au_{10}$ cluster-4			-0.68
$Au_{10}$ cluster-5			-0.61
$Au_{10}$ cluster-6			-0.58



Table S7. The adsorption energies per Au atom for Au<sub>10</sub> cluster anchoring on different functionalized MXene.

Anchoring configuration	Top view	Side view	Substrate Top view	Substrate Side view	Adsorption Energy (eV)
Bare substrate					-1.24
Au/MXene					-0.80
Full O covered					0.49
Full F covered					0.51

Table S8. The free energies per O atom adsorb on the different sites of Ti<sub>2</sub>CO<sub>2</sub> and Au cluster, respectively.

O atom on Ti <sub>2</sub> CO <sub>2</sub>	G <sub>O</sub> (eV)	O atom on Au cluster	G <sub>O</sub> (eV)
Top view	Substrate	Top view	Side view
	-1.94		2.03
	-1.92		2.14
	-1.99		2.93

Table S9. The free energies per H atom adsorb on the different sites of isolated Au cluster and Au/Ti<sub>2</sub>CO<sub>2</sub>, respectively.

H atom on isolated Au cluster	G <sub>H</sub> (eV)	H atom on Au/Ti <sub>2</sub> CO <sub>2</sub>	G <sub>H</sub> (eV)
Top view	Side view	Top view	Side view
	0.45		0.77
	0.68		0.61
	0.46		0.35
	0.54		0.22

Table S10. The total energies of COOH and HCOO intermediates on different sites of Au/Ti<sub>2</sub>CO<sub>2</sub>.

Top view	Side view	Energy (eV)	Top view	Side view	Energy (eV)

		-712.80			-711.51
		-712.06			-712.37
		-712.06			-712.44
		-711.95			-712.50
		-711.28			-712.37

Table S11. The adsorption energies of CO and H<sub>2</sub>O molecules on different sites of Au/Ti<sub>2</sub>CO<sub>2</sub>.

CO top view	CO side view	E <sub>CO</sub> (eV)	H <sub>2</sub> O top view	H <sub>2</sub> O side view	E <sub>H2O</sub> (eV)
		-0.71			-0.03
		-0.58			-0.11
		-0.52			-0.13
		-0.50			-0.16
		-0.49			-0.26

Table S12. Calculated activation barriers and reaction energies of WGS reaction for water-assisted associative pathways on a mixture terminated Au/M<sub>n+1</sub>X<sub>n</sub>T<sub>2</sub>.

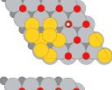
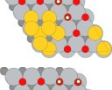
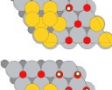
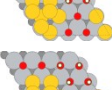
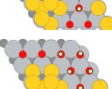
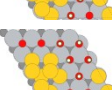
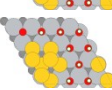
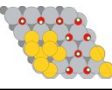
MXene	*CO → *COOH		*COOH → *CO <sub>2</sub>	
	E <sub>a1</sub> (eV)	ΔE <sub>1</sub> (eV)	E <sub>a2</sub> (eV)	ΔE <sub>2</sub> (eV)
Au/V <sub>2</sub> CO <sub>2</sub>	0.28	-0.19	0.06	-0.36
O + F (site 1)	0.30	-0.13	0.07	-0.31
O + F (site 6)	0.28	-0.20	0.04	-0.36
O + F (site 5, 6)	0.27	-0.21	0.05	-0.35
O + F (site 1, 4)	0.30	-0.10	0.07	-0.27
O + F (site 2, 3)	0.30	-0.09	0.08	-0.26
Au/Ti <sub>2</sub> CO <sub>2</sub>	0.23	-0.16	0.16	-0.09
O + F (site 1)	0.29	-0.11	0.16	-0.09
O + F (site 6)	0.27	-0.16	0.16	-0.16
O + F (site 5, 6)	0.28	-0.13	0.15	-0.11
O + F (site 1, 4)	0.32	-0.06	0.16	-0.09

<i>O</i> + <i>F</i> (site 2, 3)	0.26	-0.12	0.15	-0.11
<i>Au/Ti<sub>4</sub>C<sub>3</sub>O<sub>2</sub></i>	0.15	-0.28	0.15	-0.12
<i>O</i> + <i>F</i> (site 1)	0.22	-0.21	0.15	-0.12
<i>O</i> + <i>F</i> (site 6)	0.18	-0.28	0.14	-0.15
<i>O</i> + <i>F</i> (site 5, 6)	0.21	-0.25	0.15	-0.15
<i>O</i> + <i>F</i> (site 1, 4)	0.25	-0.16	0.16	-0.10
<i>O</i> + <i>F</i> (site 2, 3)	0.21	-0.20	0.15	-0.12

Table S13. The free energies, ZPE corrections, and entropy corrections used for the WGS intermediates.

Species	Free energy (eV)	ZPE (eV)	Entropy (eV)
CO*	-15.445	0.175	0.133
COOH*	-27.035	0.617	0.245
H <sub>2</sub> O*	-13.873	0.621	0.167
CO <sub>2</sub> *	-22.880	0.312	0.192

Table S14. The free energies of H atoms on Au/Ti<sub>2</sub>CO<sub>2</sub>.

Top view	Side view	ZPE (eV)	Entropy (eV)	Free energy of all H atoms (eV)	Free energy per H atom (eV)
		0.295	0.013	0.348	0.348
		0.587	0.027	0.752	0.376
		0.874	0.043	1.220	0.407
		1.158	0.059	1.696	0.424
		1.444	0.076	2.244	0.449
		1.737	0.092	2.737	0.456
		2.019	0.112	3.390	0.484
		2.299	0.132	4.046	0.506
		2.571	0.155	4.774	0.530